Seasonal Structure of a Simple Monsoon System

PETER J. WEBSTER

CSIRO Division of Atmospheric Physics, Mordialloc, Victoria, Australia 3195

LANG C. CHOU

Department of Meteorology, Naval Postgraduate School, Monterey, CA 93940

(Manuscript received 28 June 1979, in final form 4 September 1979)

ABSTRACT

With a structure based on observational studies which indicate that the monsoon occurs on extremely large spatial scales and shows distinct seasonal character, a model is developed with the aim of discerning the basic driving mechanisms of the mean seasonal monsoon. It is argued that for the macroscale monsoon an appropriate facsimile is a zonally, symmetric, moist and primitive equation atmosphere coupled to an interactive and mobile ocean. Via experimentation with the model a hypothesis is tested which states that the character of the mean seasonal monsoon is determined by an interplay between the basic drive of the monsoon system (i.e., the differential heating between an *interactive* ocean and continental regimes) and the hydrologic cycle.

A seasonal structure of a simple monsoon system was developed and its character discussed. With full hydrology and an ocean-continent differential heating, the model displays many features of the observed mean monsoon. Comparisons between moist and dry and oceanic and ocean-continental systems indicate the importance of the various mechanisms of the monsoon circulations. For example, scale contraction is noted with the introduction of moist processes and simple arguments are introduced to explain the scale change.

It is shown that the mean summer structure of the model monsoon is made up of low-frequency variations or transients which occupy a large fraction of the variance. The manner in which the model will be used to investigate the monsoon transients is discussed.

1. Introduction

Despite severe restrictions in data coverage in the ocean areas to the south of India, the structure of the Asian monsoon has received considerable attention. So important is the determination of the basic mechanisms which drive the monsoon circulation (an importance emanating from the social-economical advantages of being able to forecast the monsoon) that it has been the subject of a number of large-scale field experiments including the International Indian Ocean Expedition (1964–65) and the Global Atmospheric Research Program's Monsoon Experiment (MONEX, 1977–79). Less effort has been made in the past with the Indonesian–North Australian and the North African monsoon systems although there is some hope that the data collected in Winter MONEX and WAMEX (West African Monsoon Experiment), both experiments having been conducted during the First GARP Global Experiment year (FGGE), will yield at least initial descriptions.

Deciphering the role of the various mechanisms which drive or influence a system is a particularly difficult task in an inherently complex structure such as the monsoon. A number of key questions emerge as critical obstacles in the path of a full description of monsoon dynamics. These are 1) the influence on the magnitude and phase of the monsoon of the heated continent, 2) the role of hydrological processes, 3) the mechanical and thermal influence of large orographic structures such as the Himalayas, and 4) the perturbation of the basic radiative forcing by variable cloud extent.

Some partial progress has been achieved in understanding the points listed above by a number of different studies although no one model has been used to investigate *all* questions. The simulation of the monsoon has been achieved by large-scale multidimensional general circulation models with some success (e.g., Hahn and Manabe, 1975). Such models include many important physical mechanisms, feedback processes and detailed spatial resolution which, unfortunately, render experimentation expensive and difficult, especially when processes are evolving over seasonal time scales. Normally, the logistical problems of the general circulation models are overcome by the development of simpler phenomenological models aimed modestly at elucidating one or a few basic physical mechanisms rather

0022-4928/80/020354-14$07.50

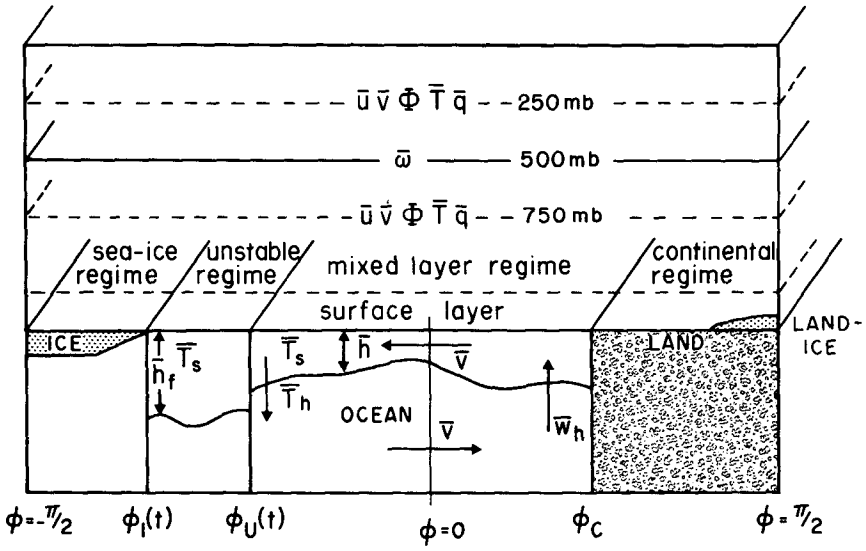

FIG. 1. Schematic representation of the interactive ocean-atmosphere model. See text for details.

than producing detailed simulations of the atmospheric structure. For example, Webster and Lau (1977, hereafter referred to as WL) and Webster (1979) studied the influence of interactive oceans on the mean seasonal and evolving seasonal flow. The model used in both studies was a dry (i.e., no hydrologic cycle) version of the domain-averaged model described in WL. They found that the magnitude and phase of the monsoon circulation was coupled directly to the lagged ocean response. Consequently, the inclusion of an *interactive ocean* in a monsoon or climate model would seem imperative. WL also showed that the formation of sea ice was an integral part of the ocean model. Without sea ice the proper phase of the latitudinal gradient of radiational heating could not be modeled.

Two important studies have aimed directly at the question of the influence of orography on the structure of monsoons. They are mentioned here to indicate the problem involved in gleaning results from different models as a means of answering the four basic questions listed above. Both Godbole (1973)[1] and Hahn and Manabe (1975), the former using a zonally symmetric model, found that orography was necessary for their monsoon simulations to resemble the observed state of the monsoon. Whereas there is apparent agreement between the two studies, substantial differences occur. On one hand, the Murakami *et al.*–Godbole study found that the *neglect* of hydrologic processes had little effect on the magnitude of the model response. On the other hand, Hahn and Manabe suggested that moist processes *in conjunction with orography* were extremely important.

In order to overcome the problem of model incompatibility and to avoid the logistical constraints imposed by a general circulation model, it would appear logical to utilize one model which would allow a rational and sequential approach to the four basic questions. Such an approach is the *aggregate method* by which the physical complexity of a model is slowly increased in successive controlled experiments. This is in contrast to the general circulation model approach where there is an attempt to include as many physical features as possible. The parent model we choose is the domain-averaged model of WL and a principal aim of this paper is to develop a rational subset of the model with the purpose of attempting to understand *the role of hydrology* in the monsoon system.

2. Model formulation

The physical structure of the model is shown schematically in Fig. 1. A zonally symmetric, two-level, nonlinear primitive equation model extending from pole to pole lies over a laterally inhomogeneous lower boundary which contains ice, ocean and land areas. The ocean surface temperature and the structure of the upper ocean are determined by the simple advective mixed-layer model of WL: The model predicts the structure of the oceanic mixed layer in stable regimes and uses convective adjustment to determine the surface temperature in unstable regions where the mixed layer is undefined. The transition point between the stable and unstable regimes is computed at each iteration. The sea and land ice extents are also predicted.

[1] Godbole's paper appears to emanate from the earlier study of Murakami *et al.* (1968). Although the latter study is a non-standard reference it is included in the References as it is an important first attempt into phenomenological monsoon studies via numerical techniques.

The continental surface temperature is determined by energy balance considerations. Vertical transports of heat, moisture and momentum are calculated using bulk atmospheric boundary-layer formulations which act as coupling mechanisms between the ocean, land and the atmosphere. The continental boundary is placed at 18°N which approximates the southern margin of the Asian land mass.

At this stage it should be pointed out that the choice of a zonally symmetric model and a particular ocean-continent geography, suggests a particular interpretation of the results. Rather than representing zonal averages, the results are more pertinent to a particular longitude belt. Such a belt would be between 60 and 100°E. Furthermore the model is developed with the aim of studying forcing and feedback processes in the tropical and subtropical region. The model thus developed will be of just that degree of sophistication to be pertinent to the tropical and subtropical latitude zones, in keeping with the aggregate philosophy.

As most of the model structure is derived from WL only certain segments of the formulation will be presented here. For greater detail, the reader is referred to WL.

a. Atmospheric model

If a zonal operator is defined such that

$$\bar{X} = \frac{1}{2\pi}\int_0^{2\pi} X d\lambda, \tag{1}$$

we can reduce a quantity X to its mean and deviation from that mean. Operating on the primitive equations in spherical coordinates, the following set emerges:

$$\frac{\partial \bar{u}}{\partial t} + \bar{G}(\bar{u}) = \bar{v}\left(f + \frac{\tan\phi}{a}\bar{u}\right) + \bar{F}_1 \tag{2}$$

$$\frac{\partial \bar{v}}{\partial t} + \bar{G}(\bar{v}) = -\frac{1}{a}\frac{\partial \bar{\Phi}}{\partial \phi} - \bar{u}\left(f + \frac{\tan\phi}{a}\bar{u}\right) + \bar{F}_2 \tag{3}$$

$$\frac{\partial \bar{T}}{\partial t} + \bar{G}(\bar{T}) = \frac{\kappa\omega\bar{T}}{p} + \bar{Q} + \bar{F}_3 \tag{4}$$

$$\frac{\partial \bar{q}}{\partial t} + \bar{G}(\bar{q}) = \bar{S} + \bar{F}_4 \tag{5}$$

$$\frac{\partial \bar{\Phi}}{\partial p} = -\frac{R\bar{T}}{p} \tag{6}$$

$$\frac{\partial \bar{\omega}}{\partial p} + \frac{1}{a\cos\phi}\frac{\partial}{\partial \phi}(\bar{v}\cos\phi) = 0 \tag{7}$$

$$\bar{G}(\bar{X}) = -\frac{1}{a\cos\phi}\frac{\partial}{\partial \phi}(\bar{X}\bar{v}\cos\phi) - \frac{\partial}{\partial p}(\overline{X\omega}). \tag{8}$$

Following usual notation, $\bar{u}$, $\bar{v}$ and $\bar{w}$ represent the eastward, northward and vertical zonally symmetric wind components and $\bar{T}$, $\bar{q}$ and $\bar{\Phi}$ the temperature, specific humidity and geopotential, respectively; $\bar{F}$, $\bar{S}$ and $\bar{Q}$ define the small-scale dissipative processes, the moisture and heat sources and sinks.

The atmospheric model was adapted to two layers in the vertical, the upper layer being centred at 250 mb and the lower layer at 750 mb. $\bar{u}$, $\bar{v}$, $\bar{T}$ and $\bar{q}$ appear as prognostic variables at both levels with $\bar{\omega}$ being calculated at 500 mb, the interface of the two layers.

The atmospheric model is a one-domain version of the multi-domain model of WL except that eddy effects are ignored, i.e., we have assumed

$$\bar{G}'(\bar{X}') = \frac{1}{a\cos\phi}\frac{\partial}{\partial \phi}(\bar{X}'\bar{v}'\cos\phi) + \frac{\partial}{\partial p}(\bar{X}'\bar{\omega}') = 0.$$

Such a relaxation is in keeping with the simplicity of the objectives of the study and with the emphasis on low-latitude phenomena.

In summary, Eqs. (2)–(8) form a closed prognostic zonally symmetric set in $\bar{u}$, $\bar{v}$, $\bar{T}$, $\bar{\Phi}$ and $\bar{\omega}$ provided that $\bar{Q}$, $\bar{S}$ and $\bar{F}$ are known. A knowledge of the latter factors requires the determination of the surface temperature which, in turn, relies on an interactive ocean and ice model.

b. Ocean and ice models

The ocean model is identical to that described in WL and is shown schematically in Fig. 1. Four basic variables define the ocean. These are a mixed-layer temperature $\bar{T}_s(\phi,t)$, a mixed-layer depth $\bar{h}(\phi,t)$, a deep ocean temperature $\bar{T}_{-h}(\phi,t)$ and a "thermohaline" circulation velocity $\bar{v}$ determined by the pressure gradient resulting from the latitudinal variation of the thermal structure. The system is closed by continuity and an assumption regarding the actual free ocean vertical velocity magnitude (see WL for details).

When $\bar{T}_s > \bar{T}_{-h}$, the ocean structure is determined by the advective mixed-layer model. Poleward of the latitude where $\bar{T}_s = \bar{T}_{-h}$ the ocean structure is modeled by convective adjustment which parameterizes the rapid downward mixing of the cold surface water, or equivalently, the upward heat flux from the warmer deep ocean. Ice is assumed to form when the upward heat flux cannot balance the heat loss at the surface. With continued cooling at the surface this must eventually occur as coupled with the convective adjustment is a deepening of the mixed layer which diminishes the efficiency of upward heat flux. Poleward of the latitude of freezing the thickness of ice is assumed to have a prescribed functional thickness.

The surface temperature of the ice surface is calculated in an identical manner to that over the land surface except that the heat flux from below the surface (F_I) is nonzero. To a first approximation, the flux of heat flux will depend on the temperature gradient across the ice ($\bar{T}_s - \bar{T}_I$), the thermal conductivity of ice (K_I) and the thickness of the ice h_I, i.e.,

$$F_I = \frac{K_I}{h_I}(\bar{T}_s - \bar{T}_I). \tag{9}$$

c. Hydrologic cycle

1) LATENT HEAT

Two parameterizations are developed for the release of latent heat by various processes. The first, large-scale condensation, permits the release when the large-scale transport of water vapor allows saturation to occur. The heating rate of the large-scale condensation is given by

$$H_L = \frac{L}{2C_p}[(q - \tilde{q}) + |q - \tilde{q}|], \tag{10}$$

where the tilde denotes the appropriate saturation value. Latent heat is thus released whenever $q > \tilde{q}$ irrespective of the column stability.

The second parameterization releases latent heat in convectively unstable regions of rising motions using a combination of the schemes of Ooyama (1969) and Anthes (1977). The convective heating rate is defined by

$$H_c = \int_{P_0}^{0} \begin{cases} \eta(1 - b)\dfrac{L}{C_p}\overline{\omega' q'}dp, & \bar{\omega} < 0 \\ 0, & \bar{\omega} \geq 0. \end{cases} \tag{11}$$

The incorporation of η and b allow effective intensity and moisture availability controls and modifies the earlier CISK (convective instability of the second kind) models of Charney and Eliassen (1964), for example. η and b will be discussed subsequently.

As the present model is constrained to two atmospheric layers, $\bar{\omega}$ in (11) is approximated by $\bar{\omega}$ (500 mb). $\tilde{q}$ is the vertically dependent moisture distribution. Thus $\overline{\omega' q'}$ is parameterized by the product of the vertical velocity $\bar{\omega}$ of the model and the specific humidity distribution. H_c is calculated as the integral over the two atmospheric layers plus the boundary layer, quantities which are calculated in the manner described in WL.

The intensity factor η was originally defined by Ooyama as the total amount of lower atmospheric air introduced into the cloud per unit mass of air from the boundary layer. Consequently, $(\eta - 1)$ units of air are entrained from the lower layer of the atmosphere. If H_i is the moist static energy of layer i $[=C_pT_i + gz_i + Lq_i]$, it can be shown from energy balance arguments of the convective updraft that

$$\eta = 1 + \frac{H_b - H_2}{H_2 - H_1} \approx 1 + \frac{\theta_{eb} - \theta_e}{\theta_{e_2} - \theta_{e_1}},$$

where θ_e is the equivalent potential temperature for the boundary layer (subscript b), the lower tropospheric layer (subscript 1) and the upper tropospheric layer (subscript 2). Our designation of η as an *intensity* factor is now obvious. With continuing convection (assuming sufficient moisture availability) stabilization occurs by the relative heating of the upper troposphere. Thus, H_2 increases which simultaneously enlarges the denominator and decreases the numerator of the expression, and η is reduced. As the moist static stabilities are prognostic functions, η places an upper bound on the maximum intensity of convection. The parameterization is similar to convection in the real atmosphere in that it takes into account the larger flux of energy that is required to be injected into the column to enable the convective updraft to be maintained in an environment of increasing stability caused by the prolonged convection.

Besides the thermal state of the atmosphere, the degree of convective activity depends on the availability of moisture. To take this into account we follow Anthes (1977) and introduce a moisture control b defined such that

$$b = \begin{cases} \dfrac{1 - R}{1 - R_c}, & R > R_c \\ 1, & R \leq R_c, \end{cases}$$

where R is the layer relative humidity and R_c a critical relative humidity defined by Anthes to be 0.5. Thus if $R < R_c$, the convective heating is assumed to be zero by (11) until the column becomes sufficiently moist by advection or local evaporation.

The hydrologic scheme also contains a consistent moisture source/sink definition for (5) such that

$$\bar{S} = C_p\left(\frac{1 - b}{b}\right)\left(\frac{H_L + H_c}{L}\right), \tag{12}$$

which allows for a realistic transport of moisture to higher levels. Precipitation is merely the integral of (12) such that

$$\bar{P} = -\frac{1}{\rho_s g}\int_0^p \bar{S}dp. \tag{13}$$

2) EVAPORATION

Bulk aerodynamical formulations are used to calculate the evaporation over the ocean surface. The evaporation is given by

$$E_0 = \rho_s|V_s|C_D(q_s - q_h), \tag{14}$$

where the subscript s denotes a surface variable

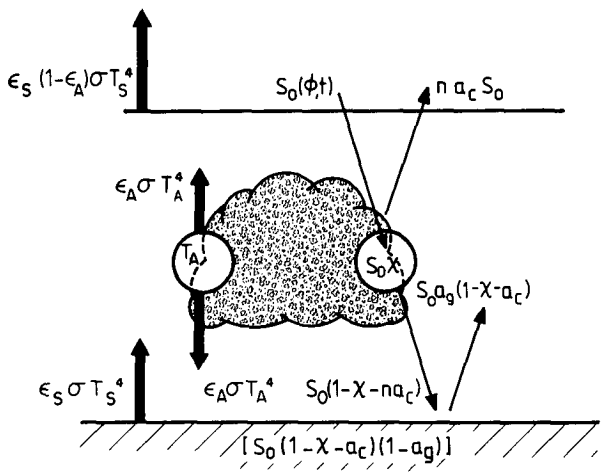

FIG. 2. Radiation model for atmosphere of cloud amount n. See text for details.

and h a variable indicative of the boundary (see WL). Over land, calculations of evaporation are identical except that the implicit assumption of an infinite evaporation source in (14) is no longer valid. The amount of evaporation will depend on the degree of wetness of the surface and the calculation of a soil moisture budget is necessary.

The method of Budyko (1974) is followed and a soil moisture W defined. If $W > W_c$, where W_c is a critical moisture content assumed to be 0.1 m, we assume that the soil is supersaturated and that the evaporation at the surface is given by (14).

If $W < W_c$, evaporation is reduced by a factor representing the moisture deficit so that

$$E = \begin{cases} E_0, & W > W_c, \quad (15a) \\ E_0 \dfrac{W}{W_c}, & W < W_c. \quad (15b) \end{cases}$$

If we define a maximum soil holding capacity W_R, we can assume that any excess moisture (i.e., $W - W_R$, if $W > W_R$) is runoff which may occur if $P > E_0$. With $W > W_R$, the rate of change of W is assumed to be zero and (15a) is invoked. If $W < W_R$, the rate of change of W is determined from the precipitation–evaporation deficit where the evaporation is calculated using (15b). In summary, the rate of change of W is given by

$$\frac{\partial W}{\partial t} = \begin{cases} 0, & W > W_R \\ P - E_0, & W < W_R. \end{cases} \quad (16)$$

d. Cloud and radiation

Recent work by Stephens and Webster (1979) indicate an extreme sensitivity of the radiative forcing of the atmosphere to the form, amount and distribution of cloud. Indeed, as an introductory example they noted the extreme longitudinal and latitudinal variability of cloud in the monsoon region and calculated the resultant variations in radiative heating. They conclude that cloud radiation-dynamic feedback calculation requires not only a detailed radiation model but also carefully construed parameterizations of the cloud production and maintenance. However, as the present model has been developed with clear and limited objectives we postpone the inclusion of fully variable clouds to a subsequent study which is assumed to be the next level of model sophistication following the philosophy of process aggregation. With the objectives in mind, we assume a constant cloud cover of 0.3 which is similar to the observed mean climatological cloud cover for the overall monsoon region.

As cloudiness is relegated to a constant value the degree of sophistication necessary to calculate the radiative forcing may be relaxed. The radiation model is an extension of Charney (1959) and matches the radiation model classification "B" of Stephens and Webster. The model structure is shown in Fig. 2 and allows for an effective atmospheric absorptivity of shortwave absorption χ and an atmospheric longwave emissivity ϵ_A. If we assume that the mean atmospheric temperature [i.e., $T_A = (T_{750} + T_{250})/2$] is equivalent to the mean radiating temperature of the atmosphere and that the radiative cooling rate Q_R of the column is equal to the net flux divergence of the column, we may write

$$Q_R = S_0(1 - na_c) - \epsilon_A(2\sigma T_A^4 - \epsilon_s\sigma T_s^4), \quad (17)$$

where ϵ_s is the surface emissivity assumed to be unity, a_c the cloud albedo (=0.6) and n the functional cloud amount (=0.3). The atmospheric emissivity and absorptivity are given values of 0.85 and 0.15, respectively. Values of the radiative parameters are consistent with those presented in Table 2 of Stephens and Webster. S_0 is the incident mean daily radiation at latitude ϕ at the top of the atmosphere so that

$$S_0 = S_{00}[(\pi/2)\sin\phi\sin\delta + \cos\phi\cos\delta]F(\sec\phi), \quad (18)$$

where $\delta = 23.45\sin(2\pi t/365)$, S_{00} is the equinoctial solar radiation incident at the top of the atmosphere at the equator, and

$$F(\sec\phi) = [0.3 + 0.7\sec(\phi - 8)]^{-1}$$

TABLE 1. Albedo law constants.

Constant	Land	Ocean
A_i	0.5	0.45
B_i	0.3	0.35
C_i	0.2	0.2
T_i	270.0	268.0

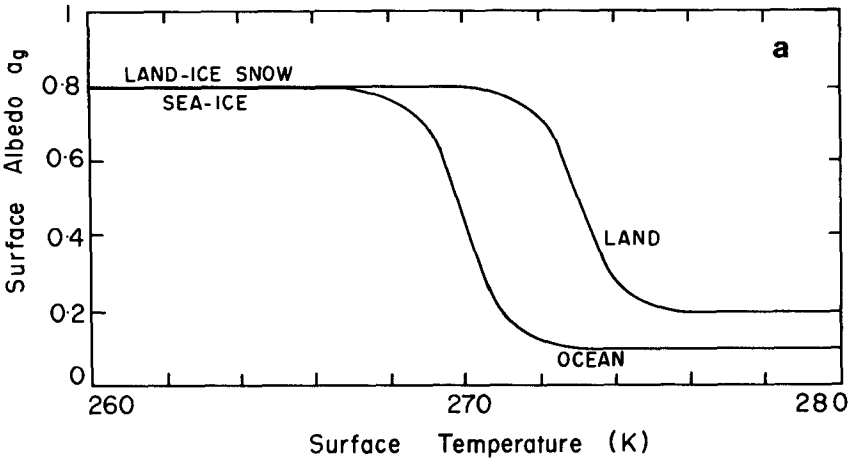

FIG. 3a. Functional dependency of albedo on surface temperature for both land and ocean surface.

where $F(\sec\phi)$ is an optical path factor and δ the solar declination angle.

The radiation model developed above differs slightly from that which is used in WL. Specifically, the longwave part of the formulation for the radiative cooling rate allows for the partial absorption of the emitted terrestrial radiation (i.e., $\epsilon_A \epsilon_S \sigma T_s^4$). With the partial opacity of the atmosphere taken into account, realistic values of atmospheric emissivities may be used (see Stephens and Webster) rather than the excessive values traditionally employed. For example, without the partial opacity (i.e., the elimination of the ϵ_A coefficient of the terrestrial longwave radiation term) values of $\epsilon_A > 1$ must be employed for balance with realistic surface temperatures (e.g., WL use $\epsilon_A = 1.02$). Thus, despite the simplification mentioned above, the radiative model provides a fair approximation to an atmosphere with constant cloud. However, in order to allow a model-produced variable cloud, the sophistication of the model must be increased—a point emphasized by Stephens and Webster.

e. Albedo formulations

As cloud and ground albedo are treated separately in the model, we deviate from WL [who used the Faegre (1972) formulation] and assume a surface albedo formulation

$$a_i = A_i + B_i \tanh C_i(T_i - T), \qquad (19)$$

where subscript i refers to the various surfaces (i.e., ocean, sea-ice, land-ice, land). The values chosen for the model are listed in Table 1. The albedo distributions shown in Fig. 3a illustrate the rapid surface albedo transition observed near the sea-ice and land-ice margins (see Budyko, 1974). To allow for the effect of ground water on the land surface albedo, an inverse dependency is introduced so that

$$a_{\text{land}} = 0.2 - 0.1\,W,$$
$$T > 273 \quad \text{and} \quad W < W_R. \qquad (20)$$

The form of a_{land} as a function of W is shown in Fig. 3b.

3. Experiments

The following initialization procedure was adopted and used in all the experiments described below. The model atmosphere was assumed to be at rest with a horizontally isothermal structure with the upper layer temperature set equal to 220 K and the lower layer to 260 K. The sea surface temperature was given by

$$T_S(\phi) = 300 - 50 \sin^2\phi \qquad (21)$$

and the continental surface temperature was set at

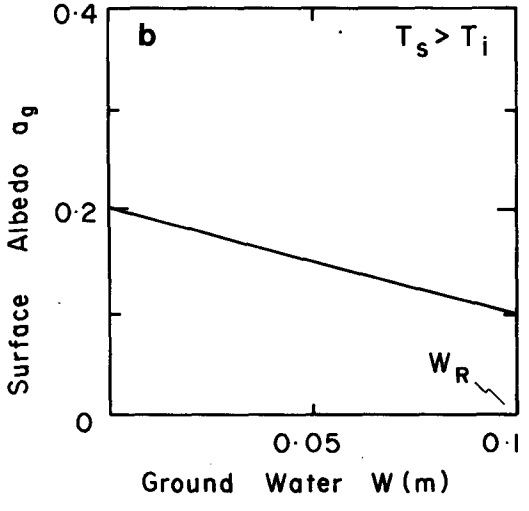

FIG. 3b. Modification of the land surface albedo by ground moisture.

TABLE 2. Properties of the various experiments.

Experiment	Label	Hydrology cycle	Geography	Integration period (years)
Dry Oceanic	DO	No	Global ocean	4
Moist Oceanic	MO	Yes	Global ocean	4
Dry Ocean–Continent	DOC	No	Continental cap $\geq$ 18°N	4
Moist Ocean–Continent	MOC	Yes	Continental cap $\geq$ 18°N	4

290 K. With an equinoctial insolation distribution maintained, the model was integrated for one year to produce an approximate steady equinoctial state which formed the initial data for all experiments. The model was then integrated for a further three years with the insolation following an annual cycle described by (18). To eliminate the effect of the transition from the initial equinoctial state to the evolving annual cycle, the mean seasonal fields were calculated from the third year of integration. Mean fields for the fourth year were quite similar but not identical.

Two sets of experiments were undertaken which involved either dry and moist conditions. In the dry case, the specific humidity was a prescribed quantity which was invariant with season, the only effect of which was in the magnitude of the atmospheric emissivity. The moist case, on the other hand, allowed the involvement of the prognostic hydrologic cycle. Each experiment was then performed for an oceanic earth and an earth containing a continental cap north of 18°N. The various experiments are summarized in Table 2.

The numerical schemes used to solve the model set

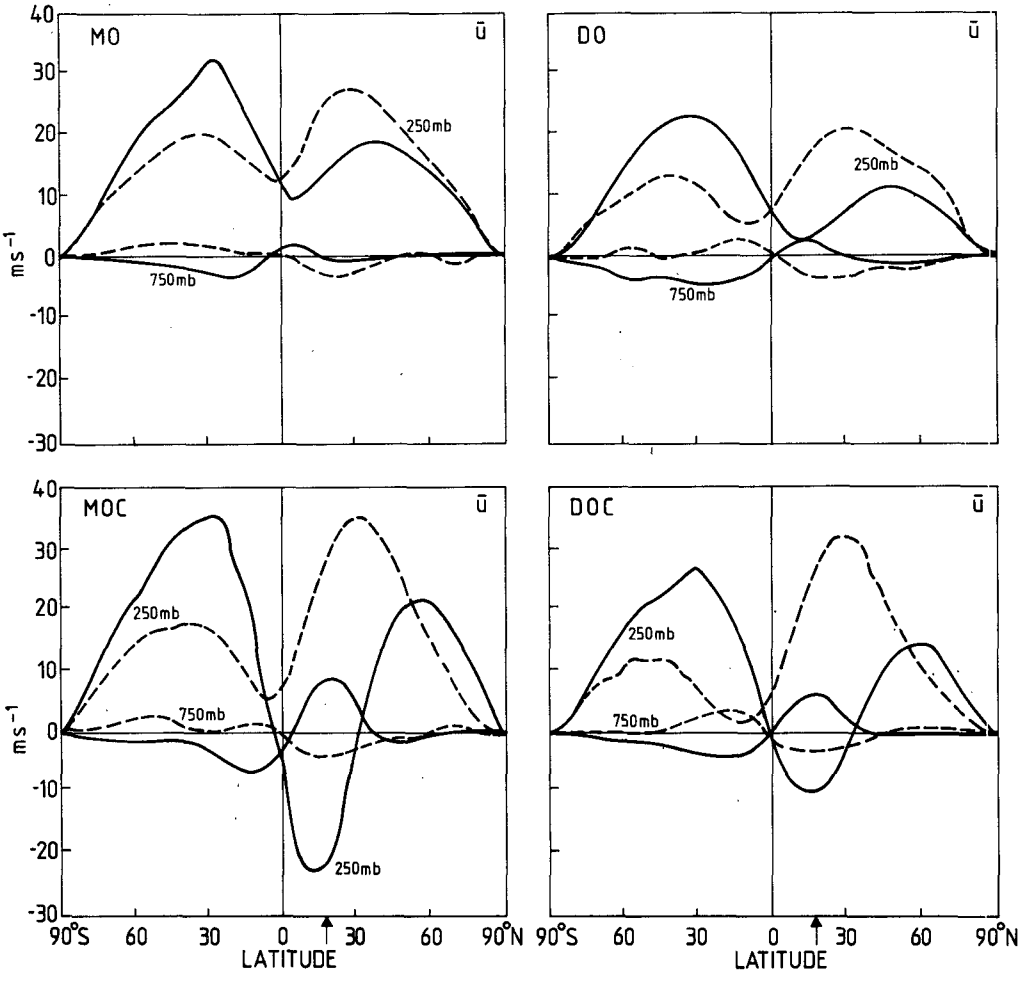

FIG. 4. Latitudinal distribution of the mean seasonal 250 and 750 mb zonal velocity component (m s^{-1}) computed for the dry ocean (DO), the moist ocean (MO), the dry ocean-continent (DOC) and the moist ocean-continent (MOC) experiments. Distributions are shown for the three month periods *following* the summer solstice (solid lines) and the winter solstice (dashed lines) of the third year of integration.

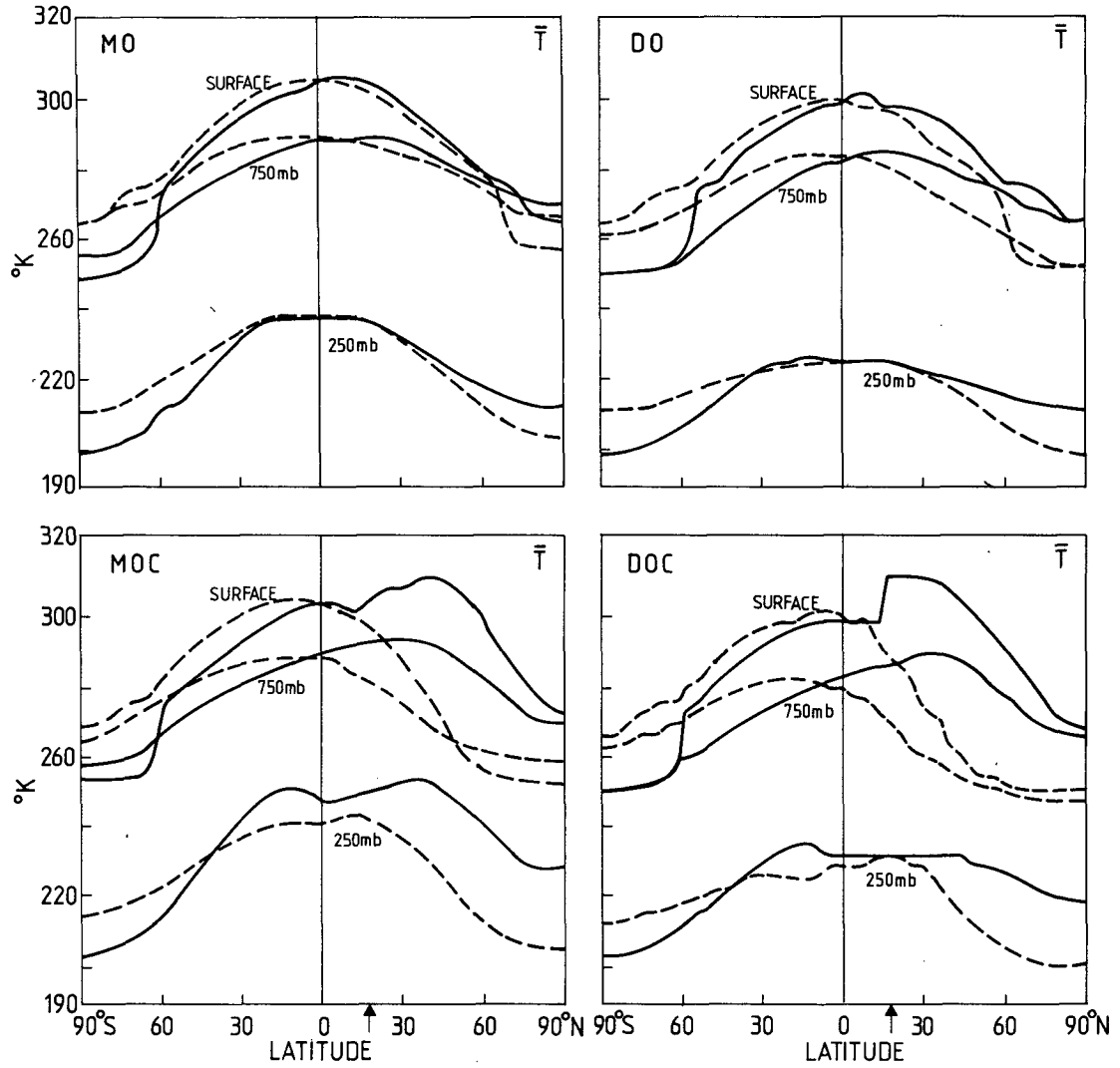

FIG. 5. As in Fig. 4 except for the mean seasonal surface, 750 and 250 mb temperature (K) fields.

are identical to those described in WL. With 80 min time steps (stable for the quasi-semi-implicit filter time-differencing scheme used) the computation time required for one simulated year of the MOC case is ~2 min on the CSIRO CDC Cyber 76.

4. Results

Figs. 4–6 show comparisons of the seasonally averaged fields of $\bar{u}$, $\bar{T}$, $\bar{\omega}$ and $\bar{v}$ for the third year of integration. Seasonal means for the fourth year were very similar. The $\bar{q}$ and $\bar{P}$ fields for the MO and MOC experiments are shown separately in Figs. 7 and 8. In each diagram the dashed curves correspond to winter season (defined as the three-month period from the winter solstice to the spring equinox) and the solid curves to the summer season (summer solstice to the autumnal equinox). As mentioned previously, the results are pertinent to the longitude belt around 80°E.

All four cases show significant individual character; the largest differences occurred between the dry and the moist experiments with the moist fields being more intense than their dry counterparts. A striking example is in the 250 mb zonal velocity field in the MOC experiment. There the equatorial easterlies are in excess of 23 m s^{-1} during the summer season compared with 9 m s^{-1} in the DOC case. Similarly, the moist vertical fields show intense narrow regions of ascending air at 10° from the equator in the MO case and over the heated continent in the MOC case, rather than the weaker and broader features of the dry experiments. Comparing the results with the observed fields presented by Webster *et al.* (1977), in particular Fig. 8, we note considerable similarity in both the magnitude and location of the mean easterly and westerly maxima.

Of all fields, only the surface temperature is stronger for the dry fields than for the moist. This is especially true over the heated continent which is

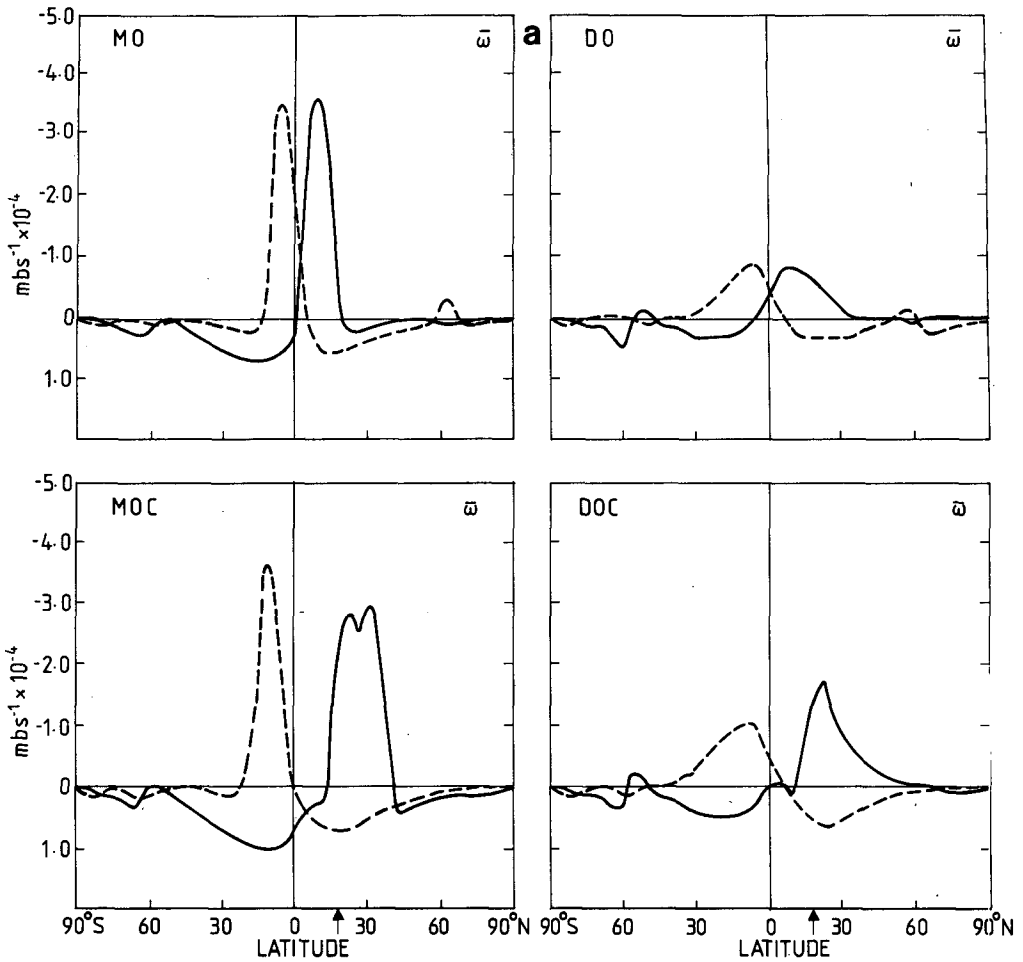

FIG. 6. As in Fig. 4 except for (a) the mean seasonal 500 mb vertical velocity (mb s^{-1}) and (b) the 750 mb meridional velocity fields (m s^{-1}).

~5 K warmer near the coastal margin. The warmer conditions can be accounted for by the absence of a hydrologic cycle and the consequent evaporational cooling from ground water accumulation. This explanation is confirmed by noting that in Fig. 5 the cooler temperatures exist only over the region of maximum precipitation shown in Fig. 8. Poleward of the precipitation peak, the continental temperature increases to near the value of the DOC experiment.

The role of moist processes is most evident in the tropospheric temperature distribution. Comparing the 250 mb temperature fields of MOC and DOC in Fig. 5 a bimodal temperature distribution may be noted about the equator. The summer maximum in the Northern Hemisphere is a result of the intense latent heating over the continental region through the entire atmospheric column and the resultant reverse temperature gradient is the cause of the strong summer easterlies to the south of the continental cap which may be seen in Fig. 4. The temperature maximum of the winter hemisphere is due to the intense subsidence (see Fig. 6) in the return leg of the meridional cell. The moist ocean case shows only a weaker version of the double upper tropospheric temperature maximum and consequently weaker (or non-existent) upper level easterlies. It should be noted that the double temperature maximum about the equator matches well the mean upper tropospheric temperatures noted by Newell *et al.* (1972) in the vicinity of the 80°E meridian. The absence of the double structure in the MO case bears a similarity to the oceanic regions of Newell *et al.*'s analyses.

Similar differences between the four experiments may also be seen in Fig. 6 which shows the vertical and meridional velocity components. For example, the moist fields are more intense and narrower than their dry counterparts as noted previously. Comparing the MOC and MO experiments, it can be seen that the winter $\bar{\omega}$ and $\bar{v}$ fields are almost identical except for a 4° poleward displacement for the MOC case. During summer the ocean-continental experi-

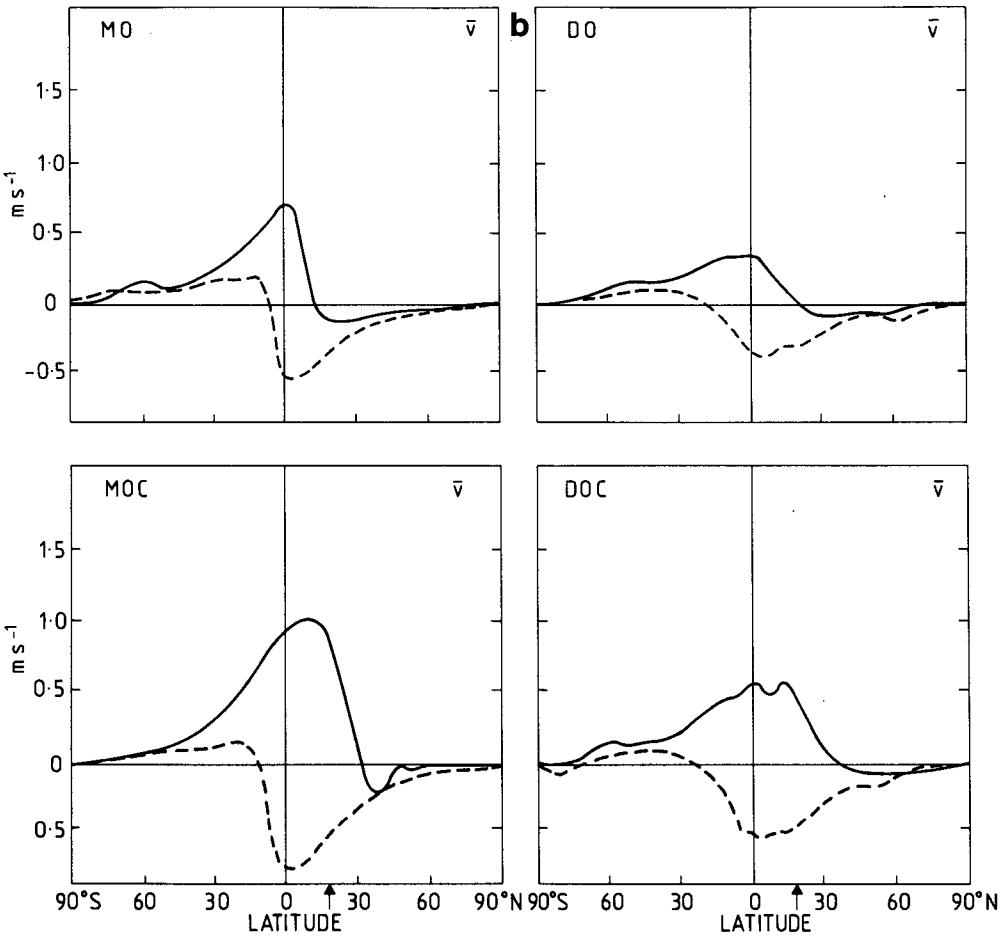

FIG. 6. (*Continued*)

ment shows a broader region of ascent over the continent, centered in the mean at ~25°N, compared to 10°N for the oceanic case. The double maximum over the continent is actually a manifestation of a substantial subseasonal variation present during the summer months. An example of the existence of the low-frequency transients may be seen in Fig. 9 which is a latitude-time plot of the 750 mb zonal velocity component.

The mean specific humidity and precipitation distributions are displayed in Figs. 7 and 8, respectively. The precipitation fields show considerable similarity to the vertical velocity fields except for the low amplitude but positive wings. Both aspects are consistent with the convective and large-scale latent heat parameterizations developed in the last section. The precipitation over land in the MOC case is considerably larger than can be accounted for solely by the vertical velocity field which, from Fig. 6, show only small differences in magnitude compared with the MO case. The reason the precipitation for the MOC case is so much greater can be seen in the considerably larger fields of specific humidity shown in Fig. 7. The difference lies in the temperature of the column in each experiment which from Fig. 5 is ~10° warmer than the MO case. Considering the simplicity of the model, the precipitation over the land area only slightly underestimates the summer precipitation in the Gangetic Plain region.

Viewed in toto the mean fields produce many interesting features, some of which bear strong resemblance to the mean fields in the vicinity of South Asia. The MO case indicates a near mirror image between the summer and winter mean vertical velocity and precipitation fields. On the other hand, the MOC case shows a strong bias in magnitude and degree of poleward penetration in the northern summer hemisphere and indicates an acute sensitivity to moisture which is particularly apparent when compared to the DOC case. That such differences occur with the inclusion of moisture is an important result as the Murakami *et al.*–Godbole study found an apparent insensitivity to the hydrologic cycle. However, by a series of experiments we have reached the contrary conclusion at least for the mean mon-

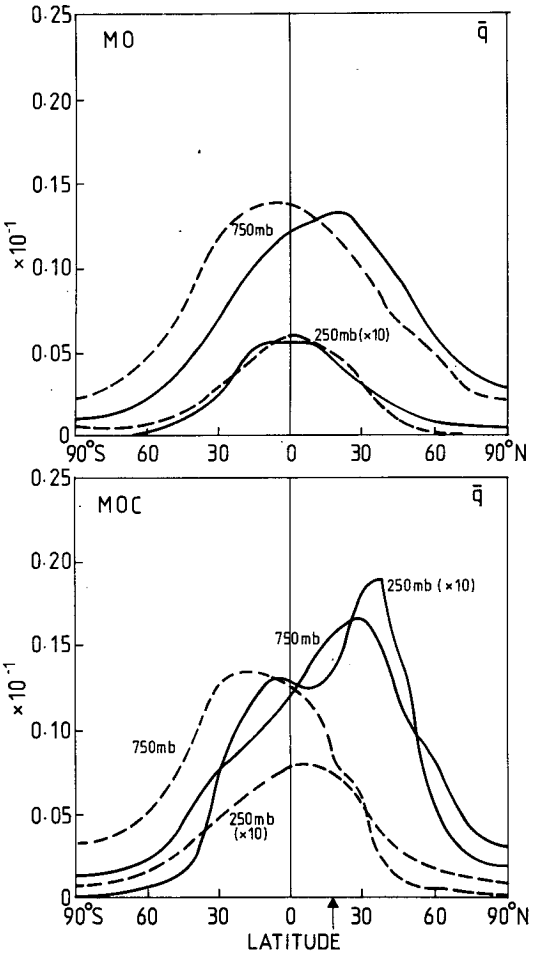

FIG. 7. As in Fig. 4 except for the latitudinal distribution of the mean seasonal specific humidity fields for the MO and MOC cases.

soon—a result which concurs with other studies of basic tropical phenomena (e.g., Charney and Elliassen, 1964; and many others).

5. Discussion

In the preceding paragraphs a number of observations were made regarding the model results and their interpretation. For completeness and in order to allow explanations to be developed of not only the mean structure of the monsoon but also, in subsequent studies, its transient state, a few of these points should be discussed.

a. Magnitude and location of the field extrema

Previously the location and magnitude of extreme mean seasonal values of some of the variables were noted. It was inferred that the mean MOC fields were complicated but recognizable combinations of the DOC and MO cases. This may be seen in the surface and tropospheric temperature distributions and their relationship to the dynamic fields. Over the ocean the temperature fields are determined by the dynamics of the mixed layer which, in turn, depend on the deep ocean temperature and the heat balance and the wind stress at the surface of the ocean. Because all four factors are involved, a considerable lag with maximum insolation occurs so that maximum sea surface temperatures generally occur between the summer solstice and the autumnal equinox. Over land the lag is considerably less and in the MOC case, two relative surface temperatures simultaneously exist (i.e., the ocean and the continental maxima) during the summer with different phases relative to the insolation. Another complicating factor is the moisture content in the continental region. As the surface temperature over land is determined by energy balance considerations, evaporative cooling (or the flux of latent heat away from the surface) is taken into account. Con-

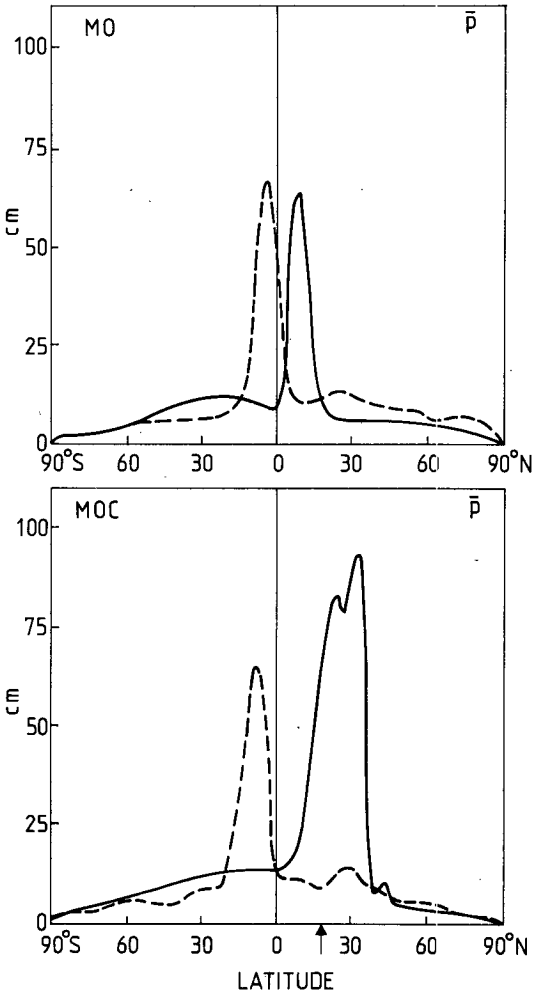

FIG. 8. As in Fig. 5 except for the latitudinal distributions of the mean seasonal precipitation (cm) for the MO and MOC cases.

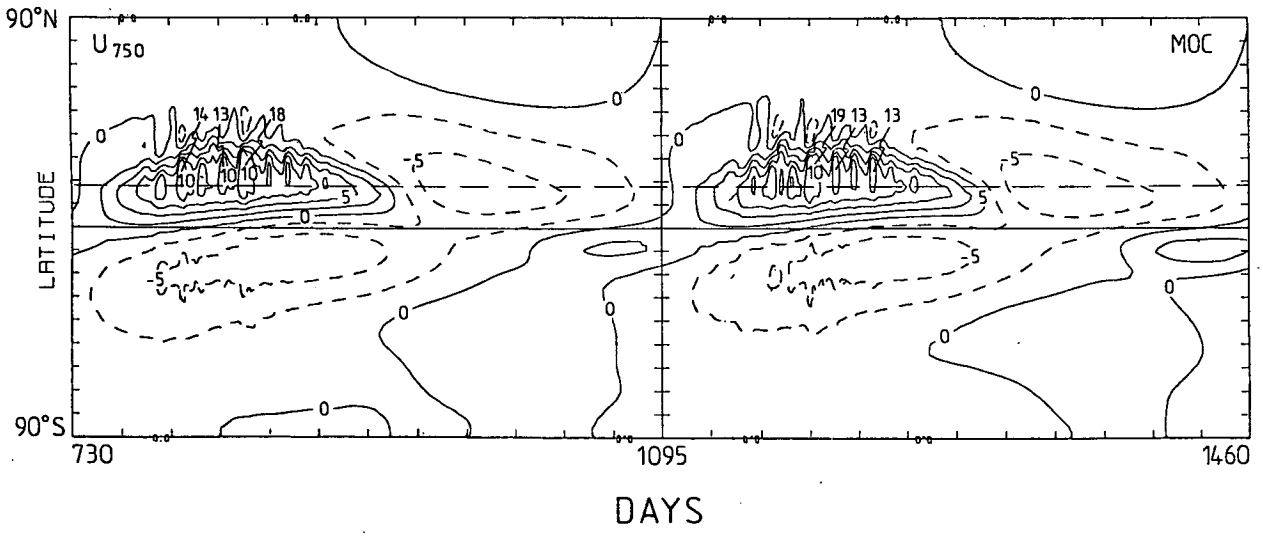

FIG. 9. Latitude-time section of the 750 mb zonal velocity component for the third and fourth years of integration for the MOC case. Units are m s^{-1} and contour intervals 2.5 m s^{-1}.

sequently, the region of maximum insolation over land need not be the region of maximum temperature as is the case in Fig. 5 for the MOC case.

The mechanisms which determine the rather complicated distribution of surface temperature are reflected directly in the dynamic structure of the model atmosphere. This may be seen from (4), the first law of thermodynamics, which may be written to good approximation as

$$\frac{\kappa \bar{T}}{P}\bar{\omega} \approx -\bar{Q}. \tag{22}$$

The equation stipulates that the vertical velocity distribution is almost determined by the heating distribution or, alternatively, that within an atmospheric column, the non-adiabatic heating is nearly completely balanced by adiabatic effects.

In both seasons of the MO case and for the winter of the MOC case, it can be seen by comparing Figs. 5 and 7 that maximum ascent corresponds to maximum surface temperature. Thus from (22) we can infer that over the ocean, maximum surface temperature coincides with maximum non-adiabatic heating. This appears consistent with the boundary heat fluxes calculated by the bulk formulations where the magnitude of the sensible heat flux is determined principally by the surface temperature (for reasonable lapse rates) as is the latent heat flux over ocean regions where the moisture source can be assumed potentially infinite. Such correspondence also follows to the DOC case where during summer maximum ascent occurs over the warmest continental region which, because the latent heat flux is zero, matches the maximum sensible heating. Only in the MOC case in summer over the continent does the correspondence between $\bar{\omega}$ and $\bar{T}_s$ fail. As mentioned previously in the MOC case the maximum surface temperature occurs well north of the coastal margin, the moist area close to the coast being cooled by evaporation. However, as evaporation is extremely large and correlates with a substantial latent heat flux, $\bar{Q}$ is largest to the south of the maximum surface temperature.

In summary, it appears that over the ocean maximum ascent will coincide with maximum surface temperature whereas over a moist continent it is constrained to lie equatorward of the warmest regions. In fact, in the MOC case the warmest regions correspond to substantial subsidence. It is interesting to note that it is only when moist processes are taken into account that regions of maximum surface temperature are subsident. This suggests that in the real atmosphere desert regions are strongly coupled to adjacent regions of convective activity. Indeed, Stephens and Webster (1979) allude to strong dependencies between the Bay of Bengal region and the desert regions to the west of the Arabian Sea based on energy balance considerations.

It should also be noted that in summer the simulated upper tropospheric temperature maximum in the Northern Hemisphere corresponds to the region of maximum heating. This provides an apparent equatorial slope with height between the surface and 250 mb of the maximum temperature which perhaps resembles the African or Australasian summer monsoon system rather than the summer South Asian system. According to Newell *et al.* (1972) the slope with height of maximum temperature is almost zero or perhaps poleward, indicating the influence of the heated Tibetan Plateau omitted in this study.

b. Scale contraction

By comparison of the results of the various experiments (e.g., MO with DO and MOC with DOC, especially in Fig. 8) it is obvious that hydrologic processes or the release of latent heat effects a diminishing or contracting of horizontal scales of motion. The scale reduction may be discussed using an even simpler model.

If A is the fractional ascending area of a region and $(1 - A)$ the fractional descending part, we may write from mass continuity

$$\frac{\omega_1 A}{\rho_1} + \frac{\omega_2(1 - A)}{\rho_2} = 0, \tag{23}$$

where the subscript 1 refers to the ascending part and 2 to the descending part. We note from observations that the horizontal temperature gradient is fairly small and again assume that the first law of thermodynamics scales as (22) and is appropriate for both the ascending and descending regions. Furthermore we assume that the nonadiabatic heating is given by

$$Q_i = S_i + L_i + R_i, \quad i = 1, 2, \tag{24}$$

where the right-hand side represents sensible, latent and radiative heating, respectively. To incorporate a latent heat release law we simplify (11) by assuming $L_1 = -\alpha\omega_1$ and $L_2 = 0$, where α is some function of the moisture field. L is then a measure of the interaction or feedback between the dynamics and convective heating.

Noting that $\rho_1 \approx \rho_2$ and using (22), (23) and (24) together with the latent heat parameterization, we obtain the following expression for the area of convection:

$$A = (S_2 + R_2)\left[(S_2 + R_2) - \frac{\kappa\bar{T}_2}{P} \times \left(\frac{S_1 + R_1}{\frac{\kappa\bar{T}_1}{P} - \alpha}\right)\right]^{-1}. \tag{25}$$

For the vertically averaged column $R_2 < 0$ and $|R_2| > S_2$ which must occur because in region 2 $\omega_2 > 0$ (i.e., subsidence). For no latent heating (i.e., $\alpha = 0$), $A \leq \frac{1}{2}$ for $|S_2| \approx |S_1|$ and $\bar{T}_1 \approx \bar{T}_2$. With latent heating ($\alpha > 0$), the denominator becomes larger and negative with substantial diminuation of A. Basically, Eq. (25) states that $A(\alpha = 0) > A(\alpha > 0)$ or, alternatively, that the stronger the heating in a column the larger the vertical velocity needed to provide a balancing adiabatic cooling which from mass continuity constrains A to simultaneously decrease.

c. Subseasonal transients

The seasonal mean fields were compiled from the evolving state of the model monsoon and are consequently comprised of transient features of various space and time scales. Fig. 9 shows an example of the transient nature of the monsoon in the form of a latitude-time section of the 750 mb zonal velocity component for the MOC experiment during years 3 and 4 of integration. Whereas the general features suggested by the mean seasonal fields are apparent in Fig. 9, one can also see considerable variation, especially in the northern summer over the continental region. Although not shown here, neither the DOC nor MO cases possess similar low-frequency transients. In a separate study aimed specifically at the transient structure of the monsoon (Webster and Chou, 1980), it is shown that the variations of the northern summer are coherent features of the monsoon and are associated with successive poleward propagations of the monsoon cell from the Northern Hemisphere ocean region to well north of the continental boundary. Such propagations appear to be related to the "break-active" monsoon sequence. In this study we merely point out that the MOC mean fields contain features of considerable variance which occur on substantial space scales with approximately a biweekly periodicity.

6. Concluding remarks

A simple model has been developed in order to form a base for a number of experiments aimed at the determination of the basic driving mechanisms of monsoon flow. In this first instance, the mean seasonal structure of a simplified version of the South Asian monsoon is studied. We have built on the results of earlier theoretical investigations (in particular WL) by adopting an *interactive* ocean and a continent, differentially heated by an evolving solar cycle, as the basic requirements for the monsoon model. In the spirit of process aggregation and phenomenological modeling, hydrology is added to the system and its effects gauged by careful control experimentation. Variable cloudiness and orography will be successively added to the system in later studies. The effects of eddies and laterally adjacent oceans, present in WL, were purposely omitted from the model in order to allow a tractable analysis of a very simple system.

Viewed from the confines of the simplified model, a number of conclusions have been reached regarding the role of hydrology in forming the mean seasonal structure of the monsoon. In Section 5 it was pointed out that both the location and magnitude of the various variable extrema were strong functions of hydrology. Interpretation of the model results allowed an understanding of the latitudinal variation of surface temperature, and the positioning of the mean summer easterly maximum. Simple thermodynamical arguments based on model results have allowed some insight into the scales of motion of moist processes. In fact, with hydrology, i.e., an interactive ocean and continentality, the results

of the simple model show unexpected agreement with the observed gross mean monsoon. Such agreement suggests that further experimentation can be approached with confidence.

The effects of neglected processes are also apparent in the model results. In particular, the neglect of eddies and the lack of their influence on the mean midlatitude motions is quite noticeable and appears responsible for somewhat weaker and less peaked westerly maxima than those observed. A better midlatitude structure was probably produced by WL who included eddy effects. The lack of eddy transports is clearly evident in the precipitation distribution (Fig. 8). In place of the observed midlatitude precipitation maximum, the model predicts a broad, low precipitation region through the subtropics and midlatitudes of the winter hemisphere caused principally by supersaturation resulting from large-scale convergence. With eddies the convergence would have occurred at higher latitudes in a considerably narrower band.

A further aim of compiling the seasonal mean fields was to gain an understanding of the results of the Murakami *et al.*–Godbole experiments. Their basic objective was to gauge the importance of the Himalayan mountains on the large-seasonal structure of the monsoon. With the orographic features included and with a hydrologic cycle, they produced fields of zonal velocity component of similar intensity and position to those shown in Fig. 4. When the mountains were neglected but hydrology maintained, the magnitudes of the zonal wind fields were reduced substantially. When hydrology alone was neglected, the fields did not appear to change. Consequently, in *sharp contrast* to the results found in the current study, both Murakami *et al.* and Godbole found the hydrology cycle to be of little importance. It is difficult to state precisely why the results of the studies should differ so greatly. However, considering the correlation between vertical velocity and condensational heating which has been established by a number of studies and demonstrated here by its effect on scale and magnitude, it is difficult to conceive of a tropical system which is effectively independent of latent heating, as suggested by Murakami *et al.* and Godbole. Unfortunately, although their results support earlier hypotheses[2] regarding the importance of the Himalayas in maintaining the mean monsoon circulation, it would appear that their relegation of relative importance between hydrology and orography must be in doubt.

Within the limits defined above, the model develops its own forcing functions and feedbacks which may exist on a multitude of space and time scales. For example, through its convective parameterization relatively rapid transients may develop. At the other end of the scale the slowly evolving interactive ocean may produce time scales which are considerably longer. The mean fields presented above are integrals of all these scales over a seasonal period and define an envelope within which the component aggregates reside. Because of this multiplicity of time scales it is an insufficient test of a model to merely examine mean fields as it is also necessary to establish that the lower frequency transients are physically reasonable. Such a test of the model which will be used for further experimentation into monsoon dynamics has been undertaken by Webster and Chou (1980).

Acknowledgments. Thanks are due to Dr. G. L. Stephens and Mr. B. G. Hunt for interesting discussions relating to the phenomena studied and the form of the final manuscript. This research was sponsored in part by the National Science Foundation, under Grant ATM 78-14821A01.

[2] In particular Flohn, 1968: Contributions to a meteorology of the Tibetan Highlands. Atmos. Sci. Pap. No. 130. Colorado State University.

REFERENCES

Anthes, R. A., 1977: A cumulus parameterization scheme utilizing a one-dimensional cloud model. *Mon. Wea. Rev.*, **105,** 270–286.

Budyko, M. I., 1974: *Climate and Life*, David H. Miller, Ed. *Int. Geophys. Ser.*, No. 18, Academic Press, 508 pp.

Charney, J. G., 1959: On the general circulation of the atmosphere. *The Atmosphere and the Sea in Motion*, Rockefeller Institute, 178–193.

——, and A. Eliassen, 1964: On the growth of the hurricane depression. *J. Atmos. Sci.*, **21,** 68–75.

Faegre, A., 1972: An intransitive model of the earth-atmosphere system. *J. Appl. Meteor.*, **11,** 4–6.

Godbole, R. V., 1973: Numerical simulation of the Indian summer monsoon. *Indian J. Meteor. Geophys.*, No. 1, **24,** 1–14.

Hahn, D. G., and Manabe, S., 1975: The role of mountains in the South-Asian monsoon circulation. *J. Atmos. Sci.*, **32,** 1515–1541.

Murakami, T., R. V. Godbole and R. R. Kelkar, 1968: Numerical experiment of the monsoon along 80°E longitude. Sci. Rep. No. 62, Indian Meteorological Department, Poona, 51 pp.

Newell, R. E., J. W. Kidson, D. G. Vincent and G. J. Boer, 1972: *The General Circulation of the Tropical Atmosphere and Interactions with Extratropical Latitudes*, Vol. 1. The MIT Press, 258 pp.

Ooyama, K., 1969: Numerical simulation of the life cycle of tropical cyclones. *J. Atmos. Sci.*, **26,** 3–40.

Stephens, G. L., and P. J. Webster, 1979: Sensitivity of radiative forcing to variable cloud and moisture. *J. Atmos. Sci.*, **36,** 1542–1556.

Webster, P. J., 1979: A model of the seasonally varying planetary scale monsoon. *Dynamics of Monsoons*, A. B. Plarce and C. D. Lighthill, Eds., Cambridge University Press.

——, and L. C. Chou, 1980: Low-frequency transitions of a simple monsoon system. *J. Atmos. Sci.*, **37,** 368–382.

——, and K. M. W. Lau, 1977: A simple ocean-atmosphere climate model: Basic model and a simple experiment. *J. Atmos. Sci.*, **34,** 1063–1084.

——, L. C. Chou and K. M. W. Lau, 1977: Mechanisms effecting the state evolution and transition of the planetary scale monsoon. *Pure Appl. Geophys.*, **115,** 1463–1491.